International Journal of Environmental Science and Technology (2024) 21:5351–5366
https://doi.org/10.1007/s13762-023-05363-0

ORIGINAL PAPER

Assessing environmental radon contribution by different sources near a South African gold mine tailings

F. S. Komati[1] · O. M. Ntwaeaborwa[2] · R. Strydom[3]

Received: 22 August 2021 / Revised: 23 June 2023 / Accepted: 14 November 2023 / Published online: 11 December 2023

Abstract

Airborne radon concentration at any given location is influenced by locally exhaled radon and dispersed radon from other locations. As a means of trying to discriminate between different radon contributors, radon gas, individual radon daughters or progenies, and the equilibrium factor were measured at different receptor points downwind and upwind of a mine tailings storage facility by following the direction of the wind at hourly intervals. The AlphaGUARD PQ2000 PRO model active radon monitor was used to measure radon concentration, and the Eberline SPA-1A alpha scintillation detector coupled to Eberline Smart Portable 2 counter was used to measure the radon daughter concentrations. The Busigin and Phillips three-count method was used to calculate the radon daughter concentrations, and hence the equilibrium factor. The minimum value of equilibrium factor was 0.016 ± 0.012 measured upwind, whereas the maximum value was 0.502 ± 0.044 measured downwind. The results revealed strong influence by external meteorological effects on the distribution of radon and radon daughters some distance from the tailings and background. The equilibrium factor, which indicates the "age" of the gas, and radon gas concentrations, increased to their highest values in the mornings when the wind was blowing from north–north-east direction. The results confirmed that concentrations of radon and its daughters do not remain constant even under same distances from a tailings or same wind speeds. Furthermore, concentration changes by radioactive decay were overshadowed by other factors such as changing wind direction and local conditions of exhalation.

Keywords Background radon · Downwind · Equilibrium factor · Meteorological conditions · Radon progeny · Upwind

Introduction

Radon (^{222}Rn) is an ubiquitous radioactive inert gas, which is a member of the Uranium (^{238}U) decay chain. In the atmosphere, radon continues to undergo spontaneous radioactive decay to produce four solid, short-lived radio nuclides or progenies, namely ^{218}Po (RaA), ^{214}Pb (RaB), ^{214}Bi (RaC) and ^{214}Po (RaC'), of which the polonium isotopes are alpha emitters, while RaB and RaC are beta emitters. Radon and its short-lived progenies, particularly the alpha emitters ^{218}Po and ^{214}Po, are considered as the major contributors to radiation exposure to humans from natural radiation, with the progenies being the dominant contributor compared to radon itself (UNSCEAR 2000, 2008).

The adverse radiological and carcinogenic effects of radon and its decay products are well documented (Thompson 2014; Bersimbaev and Bulgakova 2015; Field 2018; Kang et al. 2019; Degu Belete and Alemu Anteneh 2021). World Health Organisation (WHO) reported that radon and its progenies are recognised as the second leading causative agent for lung cancer after tobacco smoking (WHO 2009). The primary pathway to radiation exposure in human lungs is through the inhalation of the short-lived radon progenies in the atmosphere and their subsequent depositions in the respiratory system. The inhaled progenies deposit in the lungs, decay and release alpha particles at high energy which may strike and damage the lung cells. Chronic exposure to radon progenies may lead to malignant transformation, eventually leading to lung cancer (Neuberger et al. 1996; Lubin

Editorial responsibility: I. Akkurt.

✉ F. S. Komati
fkomati@cut.ac.za

[1] Department of Mathematical and Physical Sciences, Central University of Technology, Private Bag X 20539, Bloemfontein 9300, South Africa

[2] School of Physics, University of the Witwatersrand, Private Bag 3, Braamfontein 2050, South Africa

[3] Parc Scientific, P O Box 1045, Cresta 2118, South Africa

et al. 2004; Darby et al. 2005; Chen et al. 2012). It is this correlation between exposure to radon and radon progenies and the induction of lung cancer that prompted the International Agency for Research on Cancer (IARC), a subsidiary of WHO, to categorise radon as Group 1 carcinogen (IARC 1988).

Over the years, gold mining operations in South Africa have resulted in millions of tons of uranium bearing rocks and undesirable radioactive materials being brought to the surface. After the milling and gold extraction processes, the uranium bearing tailings are disposed as waste on large tailings dams. The existing and widespread environmental distribution of uranium and its decay products from the tailings pose a major environmental radiation contributor (Siaway et al. 2009; ATSDR 2012) and have the potential to fractionally increase public exposure to radon and its progenies beyond recommended levels. Due to its relatively long half-life of 3.8 days, the radon gas is carried long distances from the tailings and potentially exists at elevated levels at receptor locations where members of the public reside, resulting in a radiological dose impact due to inhalation.

Given its terrestrial origins, radon gas also exhales from almost all soil surfaces on earth. This leads to an ambient or background radon concentration which exists at various levels at any location, irrespective of the presence of anthropogenic radon sources like tailings dams. As a result, a measurement of radon gas concentration in air at a public location cannot differentiate between natural background radon and radon from a Technologically Enhanced Naturally Occurring Radioactive Material (TENORM) facility like a tailings dam in the near vicinity, and only yields the total radon concentration. Nuclear regulations require mine operators to assess the radiological impact of their operations on members of the public. In terms of radon gas, the impact relates to the radon concentration increase caused by the operation, which cannot be differentiated by direct radon gas measurements.

Previous studies (Singh et al. 2005; Arnold et al. 2009; Tchorz-Trzeciakiewicz and Solecki 2018) have shown that dilution factors like radioactive decay, which in turn depend on time, height, and place, can also change radon exhalation rate and radon concentrations at sampling point. In addition, radon concentration and equilibrium equivalent radon concentration (EEC) tend to decrease notably with time and distance from the source (tailings) and depend on climatic and meteorological factors (Momeni et al. 1979; Baciu 2005; Molchanov et al. 2010; Moshupya et al. 2019). The concentration of radon at any given location is influenced by two factors: (a) locally exhaled radon and (b) dispersed radon from other locations. In general, a single source cannot be assigned to be the only contributor to high outdoor radon concentrations (Pressyanov et al. 1995; Chambers et al. 2014). Therefore, measurements of individual radon progeny concentrations, and hence the radon equilibrium factor (F factor), may serve as good indication of the origins of the measured radon gas. These measurements contain information of the "age" of the radon gas, from which the origin of the measured radon gas can be deduced. Also, these data may be indicative of the radon gas transported from other regions.

After exhalation from both the background and the tailings, radon and its daughters are vertically transported, mixed in the boundary layer and are subjected to vertical and horizontal dispersion by the wind (Moshupya et al. 2019). A particular challenge is to isolate different radon contributors at a measuring point and to distinguish the tailings-related radon concentration in air from the background concentration. This discrimination is particularly important for radon monitoring protocols since dose limits only apply to radiation exposure exceeding background levels (ICRP 2009; Habib et al. 2018). To overcome this challenge, this study postulated that radon migration and decay are functions of distance and time. That is, "fresh" radon from the source (tailings) will decay with time and migrate to a receptor point, producing daughters/progenies and at the same time getting mixed with radon and radon daughters from other sources that have been either dispersed by the wind or locally produced from the soil. Furthermore, mixing of "old" air from the tailing and "fresh" air from other contributors can affect the quantity of the radon daughters (Leach and Chandler 1992).

In South Africa, there is limited literature available on radon exposure (Lindsay et al. 2008; Moshupya et al. 2019) from direct radon gas measurements and related radon exhalations rates from gold mine tailings (Speelman 2004; Lindsay et al. 2004; Ongori et al. 2015). Other studies and surveys on radon concentrations levels and radon dispersion from mining related facilities are commissioned by the mining companies. In essence, these studies and their results are the propriety of those regulated mining companies.

In summary, the main objective of this study was to determine the contribution of the tailings dam and other radon sources to the total radon activity concentration at a chosen location at various distances from the dam under different conditions. This gave an indication of the age of radon at each receptor point with high F factor indicating old gas and low F factor fresh gas. Under low F factor, radon is assumed to be predominantly of local origin, while high F factor indicates radon transported from distant sources. This study could contribute towards improving the understanding of the behaviour of outdoor radon and its progenies.

The study was conducted over 5 days from 19–27 August 2017, on a selected tailings dam situated in the Lejweleputswa District Municipality, Free State Province, (South Africa) between Odendaalsrus (− 27°51′59.99"

S 26°40′59.99" E) and Allanridge (27°45′15.52"S, 26°38′37.75"E) towns.

The present research was originally conducted as part of the author's thesis work (Komati 2020) at the Central University of Technology, Bloemfontein. The methods, results and analysis thereof were developed in Komati (2020) and are ingeminated and extended in this manuscript.

Materials and methods

Study area

A representative and isolated tailings dam was selected for the study. The tailings dam contains gold mine tailings from an old, non-operational closed mine shaft situated on the south of tailings dam. The dam is in Lejweleputswa District Municipality, Free State Province, (South Africa) between Odendaalsrus (-27°51′59.99" S 26°40′59.99" E) and Allanridge (27°45′15.52"S, 26°38′37.75"E) towns. The study location is shown in Fig. 1. The tailings dam is surrounded by a township on the north, R30 main road as well as maize farm on the west, a small water pond and a hostel accommodating about two hundred people on the south-east of the tailings. The closest tailings dam is about 5 km on the north-west of the tailings. This tailings dam is still "active" with wet slurry from the adjacent operating gold mine. Other tailings dams are 8.6 km and 16 km on the south and south-east side of the tailings, respectively. There are no tailings dams or other anthropogenic sources on the north, north-east and east of the dam.

The climate in Odendaalsrus is referred to as a local steppe climate, and the Köppen–Geiger climate classification is cold semiarid climate (BSk). The area receives on average, about 554 mm of rain per year, with most rainfall occurring mainly during mid-summer. August is the driest month with an average rainfall of 8 mm, and January is the wettest with an average rainfall of 93 mm (Climate-Data.org 2019). The average midday temperatures for Odendaalsrus range from 17 °C in June to an average of 30 °C in January. The region is the coldest during June/July when the mercury drops to 1 °C on average at night (Climate-Data.org 2019). The annual predominant wind directions are the north–north-east (10.8%), north–north-west (9.4%), west-north-west (9.1%), north-west (8.7%) and north (8.4%). Seasonally, the dominant wind direction during summer is the north–north-east, while during cold winter months, the wind direction varies between west-north-west and north-east (Windfinder.com 2019).

The study required detailed information about site specific meteorological conditions. For this reason, five-minute weather data from 19–27 August 2017 for the Welkom–Odendaalsrus region were obtained from the South African Weather Service (SAWS). The meteorological wind roses covering the whole study time domain are shown in Fig. 2.

The area was characterised by the dominating average wind from the north, north-east and north-west during the winter months from June to August. The predominant directions were north-east for day 1 (100%) and day 4 (100%), north for day 2 (50%), and north-west for day 3 (100%) and day 5 (90%). Wind speeds for the area varied between 1.5 m/s (day 5) and 10.80 m/s (day 4) with

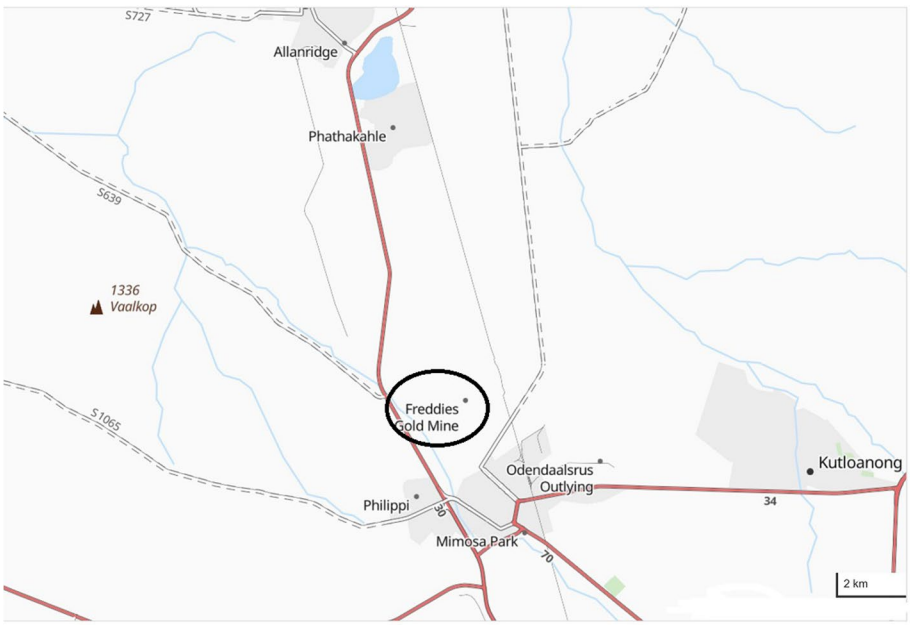

Fig. 1 Tailings' location indicated by a circle on the map (Michelin 2022)

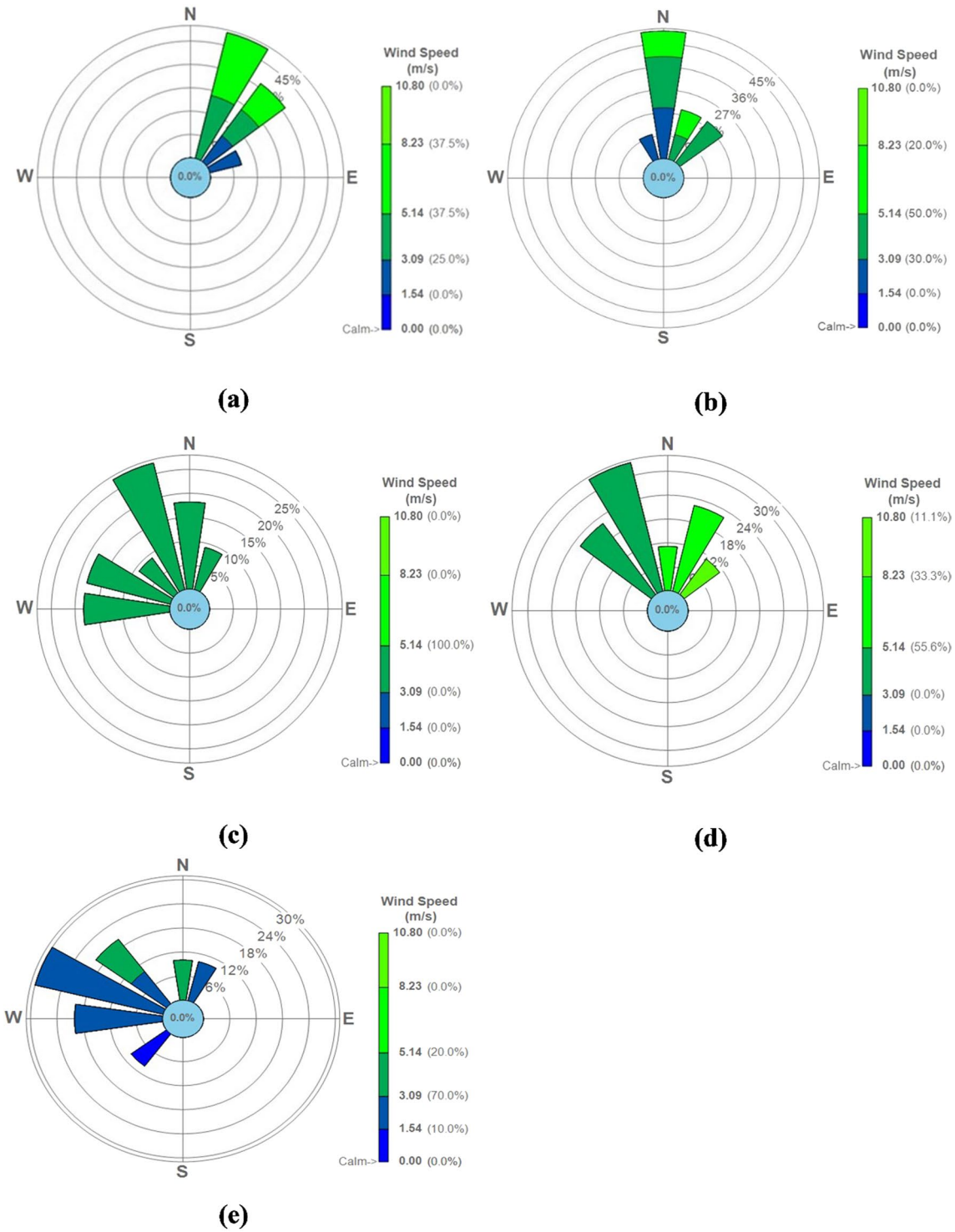

Fig. 2 Wind roses for the period 19 – 27 August 2017: (**a**) day 1(19/08/2017); (**b**) day 2 (20/08/2017); (**c**) day 3 (21/08/2021); (**d**) day 4 (26/08/2021) and (**e**) day 5 (27/08/2021)

calm periods (< 1.5 m/s) occurring for 10% of the time and wind speeds higher than 10.8 m/s occurring 11.1% of the time. The high wind speeds were mostly associated with winds from north-east, while the low wind speeds were associated with winds from north-west. Average daily minimum and maximum temperatures ranged from 9 to 20 °C during data collection period. There was no rainfall during this period.

Development of protocol for measurement of outdoor radon and radon daughters

To differentiate radon contributors, this study applied a strategy called "follow the wind" to measure radon and radon daughter concentrations at different receptor points. Radon and daughter concentrations were measured both downwind and upwind by following the direction of the wind, starting at the point closest to the tailings (source). Considering that the outdoor F factor depends on wind velocity and travel time from source of "fresh" radon to receptor point and other distances from the source, radon and radon progeny concentrations in air were, respectively, measured and collected simultaneously at time intervals of about 1 h between successive measurements from the base of the tailing. The distances between measurements varied between 100 and 200 m, depending on accessibility and suitability.

To examine the extent to which background sources might influence radon concentration, and hence that of the progenies at each receptor point, modified and simplified Bateman differential equations (Bateman 1910) called recurrence equations (Maiello and Hoover 2010) were applied to predict concentrations of radon decay and build-up of radon daughters at each successive receptor point. The use of these calculations considered only the decay of radon over time and distance by assuming that the radon originated from the tailings. This served to eventually highlight the significant effects of meteorological conditions, dispersion, dilution, mixing, etc., on radon and radon progeny transport from the tailings to the receptor. The calculated radon and progeny concentrations for each successive point were compared with the measured values. Only day 1 morning results were compared.

To minimise atmospheric removal of radon daughters by deposition process, measurements were taken during the winter month of August 2017, when the weather was dry and wind patterns relatively stable. The study postulated that during winter period, radon daughters will likely lead to high equilibrium concentrations due to trapped radon under the inversion layer. This would mostly apply to night-time and early morning conditions. The samplings and measurements for both downwind and upwind were taken in the mornings and afternoons over a period of five days. Morning samples were generally taken between 7:50 am and 12:00 am, whereas the afternoon samples were carried out between 13:00 and 16:30. For each sampling and measurement session, the initial sampling point was taken as the point closest to the dam, followed by subsequent measurements applying the "follow the wind" approach. The sampling locations were evaluated in terms of the position and meteorological characteristics of wind velocity and direction relative to the dam.

Sampling points

Figures 3 and 4 depict sampling points for downwind and upwind measurements, respectively. Taking downwind measurements, the first sampling point was chosen as the point closest to the tailings (point A), where radon activity was expected to be high in the downwind direction (Raviart et al. 1996). At this point, the radon gas from the dam was considered to be relatively "fresh", and although it represented radon from all sources, the predominant source was assumed to be the tailings dam. Therefore, point A was assumed to be characterised by very low or no activity of RaA, RaB and RaC, high radon gas activity and low F factor in the morning (Akber and Pfitzner 1994). Higher F factor values were expected in the afternoon due to radon transport from other sources, mixing and longer daughter ingrowth duration, thus rendering the gas "old" (Porstendörfer 1994; Raviart et al. 1996; Porstendörfer and Gründel 2005). In addition, stronger mixing and dilution during the day may further lead to lower afternoon radon activity levels (Song et al. 2015; Kumar et al. 2016; Čeliković et al. 2022).

After 10 min of simultaneous sampling for both radon gas and radon daughters at point A, followed by gross alpha counting, the second sampling point B was located after following the direction of the wind some distance from point A. The wind direction was determined using a light flag mounted on a car and the direction of movement of scattered soil dust and tailings. A similar follow the wind approach was applied at points C, D and E. The same procedure was followed upwind (Fig. 4). Seven sets of downwind data were taken, three in the mornings and four in the afternoons. Similarly, three sets of upwind data were taken, two in the mornings and one in the afternoon.

Sampling measurements

Radon concentration

Radon concentration sampling measurements were carried out with AlphaGUARD PQ2000 PRO pulse ionisation chamber (Saphymo GmbH, Frankfort, Germany). The AlphaGUARD, which can be operated in diffusion or flow mode with linear response from 2–2 000 000 Bq/m^3, provides high detection efficiency (5 cpm at 100 Bq/m3 (3 pCi/L)) and an instrument calibration error (Type B) of 3% (plus uncertainty of the primary standard) (Saphymo GmbH 2012). The active radon monitor was operated in flow mode with 10-min cycles, corresponding to 10-min sampling period for the radon daughter measurements. The acquired data were stored and treated with DataExpert software.

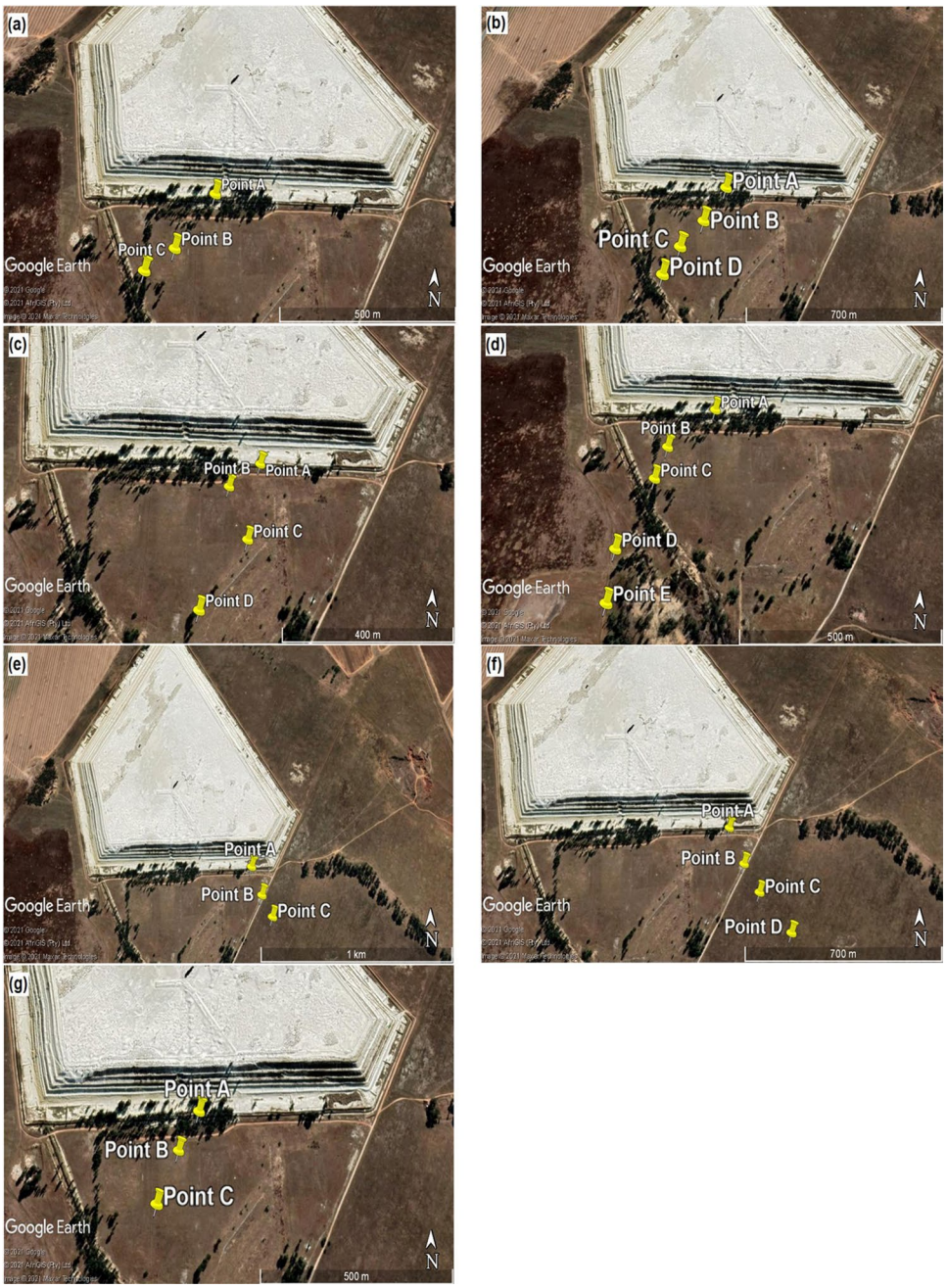

Fig. 3 Sampling points for downwind measurements and their positions and distances from the tailings

Airborne radon daughter sampling measurements

A 0.8 µm Mixed Cellulose Ester (MCE) plain white filter membrane 25 mm in diameter (Zefon International®) and 25-mm-diameter pure cellulose filter supporting pads were encased in 25 mm leak free Sensidyne® polystyrene cassette housings in an "open face" arrangement. A Dwyer RMA-22-SSV 2-inch Scale, Stainless Steel, 2–25 L per minute (LPM) airflow meter attached to a portable, DC 12 V battery operated Rocker 300DC oil-free vacuum pump (Rocker Scientific, Ltd) was connected to the filter containing cassette through the outlet to measure the flow rate. An air control valve was attached between the pump and the airflow meter to regulate the flowrate from the pump.

Prior to filter sampling and analyses, a one-minute gross alpha background count was performed on a new filter paper to check for the instrument uncertainties and to determine and quantify any alpha activity that could be present before sampling. The value obtained was then used as a background count in the calculation of radon daughter concentrations. After the background check, airborne daughter particles were collected on a filter paper by drawing air through the filter using the vacuum pump at a height of about 1 m above the ground. The air flow rate was kept constant at 14 L/min

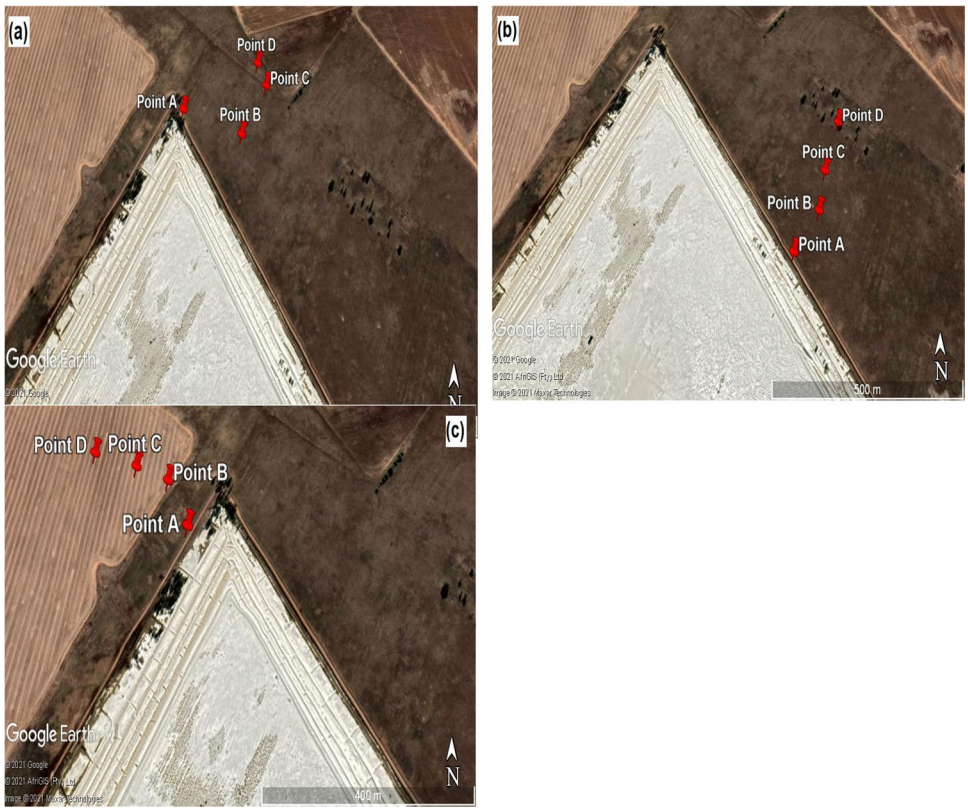

Fig. 4 Sampling points for upwind measurements and their positions and distances from the tailings

for a sampling duration of 10 min. A stopwatch was used to measure both the sampling times and counting intervals.

Filter activity measurements

For alpha counting, the filter was carefully removed from the sampling head using a tweezer and inserted inside a 0.15-cm-deep × 2.54-cm-diameter O-ring sealed slider tray sample holder of the Eberline Model SPA-1A ZnS(Ag) scintillation detector within 2 min at the end of sampling. The filter containing Eberline Model SPA-1A scintillation detector was connected to the Eberline Smart Portable (ESP-2) counter of known efficiency (60%) with a MHV (CA-15–60) coaxial cable to measure the alpha activity of the daughter particles deposited on the filter paper during sampling. The counter was operated in the Integrated Scaler mode to yield total gross counts in the specified time interval. The factory calibrated ESP-2 can store up to three sets of detector calibration parameters, rendering the instrument ready for immediate use. However, to verify if the correct calibration parameters corresponding to the Eberline Model SPA-1A scintillation detector were the same as those supplied on the Calibration Certificate, the calibration parameters were re-entered into the ESP-2 before it could be used.

Following calibration, the ESP-2's response to a check source was tested with an Americium-241 reference source to ascertain acceptable operation. The expected number of counts on the source was 1410 counts per five minutes, while the measured five-minute counts were 1250. This produced a variation of ± 11% which was considered acceptable. Therefore, the systematic error associated with this variation was calculated to be ± 11%. To further evaluate the precision of the ESP-2 alpha counter's performance, and to test the reproducibility of the results, chi-square (χ^2) test was performed on the instrument. The chi-square (χ^2) value is acceptable if it falls between 3.33 and 16.92 for a set of 10 measurements as prescribed in the (IAEA 1991). The chi-square value was found to be 8.10, which is between acceptable ranges for the counter to be considered as performing well (Paula et al. 2020).

To calculate the individual RaA, RaB and RaC radon daughter concentrations in Bq/m^3, the modified and optimised Thomas (1972) equations that correspond to the counting interval of 2 – 5, 7 – 15, and 25 – 30 min for sampling period of 10 min as proposed by Busigin and Phillips (1980) were applied. This optimised Thomas method put more emphasis on the determination of RaA, the first radon decay daughter which is an important indicator in determining the "age" of the gas at a given receptor point.

The three sets of Busigin and Phillips (1980) equations modified and corrected by Deyuan (1991), which include the background term in Bq/m^3, are:

$$C_{218_{Po}} = \frac{1}{FE}\left[6.2241C_1 - 4.231C_2 + 3.441C_3 - 2.0247R_b\right] \quad (1)$$

$$C_{214_{Pb}} = \frac{1}{FE}\left[-0.03019C_1 - 0.91247C_2 + 2.6563C_3 - 5.8913R_b\right] \quad (2)$$

$$C_{214_{Bi}} = \frac{1}{FE}\left[-0.80797C_1 + 1.68C_2 - 1.7755C_3 - 2.1388R_b\right] \quad (3)$$

where F is the flow rate in L/min; E alpha counting efficiency (60%) in cpm/dpm; R_b background count rate in cpm; C_1 gross count in interval 2–5 min after sampling (3-min count); C_2 gross count in interval 7–15 min after sampling (8-min count); and C_3 gross count in interval 25–30 min after sampling (5-min count).

Radon F factor determination in outdoor air

The radon EEC is defined as the equivalent concentration of the decay products that is in equilibrium with the parent radon having the same total potential alpha energy concentration (PAEC) per unit volume as the existing non equilibrium mixture. UNSCEAR (2000) provided the following expression for computing EEC:

$$EEC = 0.105\left(C_1\right) + 0.515\left(C_2\right) + 0.38\left(C_3\right) \quad (4)$$

where (C_1), (C_2) and (C_3) are outdoor concentrations of ^{218}Po, ^{214}Pb and ^{214}Bi, respectively, in (Bq/m^3). The F factor can then be calculated from the equation (UNSCEAR 2000):

$$F = \frac{EEC\left(Bq/m^3\right)}{C_R\left(Bq/m^3\right)} \quad (5)$$

where C_R is the radon concentration.

It has been shown that for short-term grab sampling measurements of couple of minutes, as was the case in this study, correlation between radon progeny concentration, EEC and radon concentration is so weak that in most instances it does not exist (Chen and Marro 2011; Rozas et al. 2016). Therefore, no attempt was made in this study to find correlations between these parameters.

Uncertainty approximations

Uncertainties and detection limits were obtained for each measurement. Combined uncertainties were evaluated using the Guide to the Expression of Uncertainty in Measurement (GUM) (JCGM 2008) by taking into consideration all sources of uncertainty: including calibration, sampling and background counting. The individual uncertainty components were combined using the law of propagation of uncertainties, and the uncertainty in the number of counts was given at 1-sigma range ($k = 1$). Therefore, the uncertainties quoted for the F factor are a combination of both systematic and statistical errors and correspond to $k = 1$. The counting uncertainties (Type A) for both the AlphaGUARD and the ESP-2 alpha counter were calculated using Poisson distribution.

Results and discussion

The results of the measured radon concentration, radon daughter concentrations, EEC and the F factors both downwind and upwind after applying the "follow the wind" method are presented in Table 1 and portrayed in Figs. 5, 6 and 7.

From Table 1, the highest downwind radon concentration of 23.38 ± 0.34 Bq/m^3 was observed on day 3 during the mid-morning hours, whereas the lowest downwind radon concentration of 4.60 ± 0.16 Bq/m^3 was observed on day 1 during the late afternoon hours. Diurnal patterns of radon activity levels have shown that maximum radon activity levels develop during the early hours of the morning, followed by a sharp decrease after around midday. This behaviour, consistent with diurnal pattern changes reported by other researchers (Porstendörfer 1994; Pressyanov et al. 1995; Blaauboer and Smetsers 1997; Porstendörfer and Gründel 2005; Podstawczyńska et al. 2010; Čeliković et al. 2022), can be attributed to temperature inversions, leading to nocturnal radon accumulation due to low mixing height. With rising temperature as the day progress, these inversions are terminated, resulting in higher turbulent mixing and lower radon concentrations.

On the upwind side, where measurements were taken against the direction of the incoming wind towards the dam, the highest (15.81 ± 0.28 Bq/m^3) and the lowest (1.480 ± 0.091 Bq/m^3) radon concentrations were recorded on day 2 and day 4 during the mid-morning and late morning periods, respectively. The measurements were taken on different days, under different meteorological conditions which may have had a direct influence on the ambient radon.

Regarding radon daughters, their concentrations in the close vicinity to the dam were too low to contribute towards attaining higher EEC values, particularly RaC. This deviation has been previously reported in the literature (Furuta et al. 2002). The EEC varied considerably at different receptor points from the dam, ranging from a minimum of 0.23 ± 0.28 Bq/m^3 in the afternoon to a maximum of 5.20 ± 0.64 Bq/m^3 during the morning on the upwind side. This observation has been further corroborated by Zhang et al. (2020). Most of the low values below 0.5 Bq/m^3 were observed in the afternoons. One possibility for very low or no RaC activity measured is that overall, the radon activity, and consequently, the radon daughter activity detected, was

Table 1 Radon and radon daughter concentrations, EEC and F factor values for the study period 19–08-2017 to 27–08-2017

Date	Time	Position	Concentration (RaA) (Bq/m^3)	Concentration (RaB) (Bq/m^3)	Concentration (RaC) (Bq/m^3)	EEC (Bq/m^3)	Average Rn (Bq/m^3)	F factor
Day 1 19–08-2017 Downwind	09:30	27°50′11"S 26°40′1" E	17.91 ± 1.90	6.35 ± 0.45	0	5.15 ± 0.44	10.25 ± 0.23	0.502 ± 0.044
	11:12	27°50′16"S 26°39′57" E	3.00 ± 1.30	0.55 ± 0.26	0.41 ± 0.34	0.76 ± 0.40	8.50 ± 0.21	0.089 ± 0.047
	12:00	27°50′18"S 26°39′54" E	2.16 ± 0.97	0.38 ± 0.20	0.05 ± 0.26	0.44 ± 0.30	8.44 ± 0.21	0.052 ± 0.036
Downwind	13:32	27°50′11"S 26°40′4" E	2.15 ± 0.84	0	0	0.23 ± 0.09	6.13 ± 0.18	0.037 ± 0.014
	14:30	27°50′15"S 26°40′1" E	7.11 ± 1.66	7.17 ± 0.51	0	4.44 ± 0.44	15.50 ± 0.28	0.287 ± 0.029
	15:26	27°50′18"S 26°39′58" E	2.23 ± 0.88	0	0	0.23 ± 0.09	6.19 ± 0.19	0.039 ± 0.015
	16:12	27°50′21"S 26°39′56" E	1.68 ± 0.85	0.50 ± 0.20	0	0.44 ± 0.19	4.63 ± 0.16	0.094 ± 0.041
Day 2 20–08-2017 Upwind	07:50	27°49′28"S 26°40′0" E	6.27 ± 1.51	1.82 ± 0.34	0	1.59 ± 0.33	13.25 ± 0.26	0.120 ± 0.025
	09:18	27°49′30"S 26°40′7" E	5.30 ± 1.27	1.71 ± 0.28	0	1.44 ± 0.28	8.44 ± 0.21	0.170 ± 0.033
	09:57	27°49′26"S 26°40′10" E	2.87 ± 2.01	0	2.53 ± 0.50	0.87 ± 0.40	12.69 ± 0.25	0.069 ± 0.032
	10:38	27°49′24"S 26°40′9" E	12.42 ± 1.61	7.39 ± 0.46	0	5.11 ± 0.40	15.81 ± 0.28	0.323 ± 0.026
Downwind	13:08	27°50′11"S 26°40′10" E	1.69 ± 0.69	0.48 ± 0.18	0	0.43 ± 0.16	10.75 ± 0.23	0.039 ± 0.015
	13:54	27°50′13"S 26°40′7" E	0	0	0.68 ± 0.24	0.26 ± 0.09	20.63 ± 0.32	0.013 ± 0.005
	14:50	27°50′17"S 26°40′9" E	3.09 ± 0.91	0.73 ± 0.20	0	0.70 ± 0.20	10.94 ± 0.24	0.064 ± 0.018
	15:49	27°50′22"S 26°40′5" E	8.04 ± 1.30	0.41 ± 0.19	0	1.06 ± 0.23	7.66 ± 0.19	0.138 ± 0.031
Day 3 21–08-2017 Downwind	07:39	27°50′11"S 26°40′0" E	17.8 ± 2.4	4.05 ± 0.47	0	3.95 ± 0.50	20.63 ± 0.32	0.192 ± 0.024
	08:35	27°50′15"S 26°39′56" E	11.8 ± 2.1	3.71 ± 0.42	0	3.15 ± 0.43	20.13 ± 0.32	0.157 ± 0.022
	09:25	27°50′18"S 26°39′54" E	12.3 ± 1.9	1.96 ± 0.35	0	2.30 ± 0.38	23.38 ± 0.34	0.099 ± 0.016
	10:28	27°50′24"S 26°39′51" E	6.2 ± 1.4	0.17 ± 0.26	0	0.74 ± 0.28	10.69 ± 0.23	0.069 ± 0.026
	11:14	27°50′28"S 26°39′51" E	6.9 ± 1.3	1.29 ± 0.25	0	1.40 ± 0.27	20.25 ± 0.32	0.069 ± 0.013
Downwind	13:00	27°50′10"S 26°40′22" E	2.03 ± 1.02	0.25 ± 0.21	0	0.38 ± 0.32	13.13 ± 0.26	0.029 ± 0.024
	13:52	27°50′12"S 26°40′27" E	3.08 ± 0.88	0.36 ± 0.18	0	0.51 ± 0.18	20.50 ± 0.32	0.025 ± 0.009
	15:24	27°50′15"S 26°40′35" E	1.52 ± 0.71	0.49 ± 0.19	0	0.41 ± 0.17	8.38 ± 0.21	0.049 ± 0.020
Day4 26–08-2017 Upwind	08:51	27°49′46"S 26°40′15" E	5.28 ± 1.33	0.98 ± 0.26	0	1.06 ± 0.27	3.80 ± 0.14	0.280 ± 0.073
	09:43	27°49′43"S 26°40′18" E	5.01 ± 1.31	0.93 ± 0.26	0	1.00 ± 0.27	8.44 ± 0.21	0.119 ± 0.032
	10:33	27°49′40"S 26°40′19" E	3.19 ± 1.09	1.51 ± 0.27	0	1.11 ± 0.25	6.91 ± 0.19	0.161 ± 0.037
	11:27	27°49′36"S 26°40′21" E	4.99 ± 1.27	0.24 ± 0.25	0	0.65 ± 0.26	1.48 ± 0.09	0.438 ± 0.177

Table 1 (continued)

Date	Time	Position	Concentration (RaA) (Bq/m^3)	Concentration (RaB) (Bq/m^3)	Concentration (RaC) (Bq/m^3)	EEC (Bq/m^3)	Average Rn (Bq/m^3)	F factor
Downwind	13:19	27°50′11"S 26°40′18" E	6.17 ± 1.23	1.53 ± 0.26	0	1.44 ± 0.26	6.19 ± 0.18	0.232 ± 0.042
	14:12	27°50′15"S 26°40′20" E	4.84 ± 1.27	1.00 ± 0.26	0	1.02 ± 0.26	13.38 ± 0.26	0.077 ± 0.019
	15:04	27°50′18"S 26°40′22" E	2.66 ± 0.92	0	0	0.28 ± 0.10	10.88 ± 0.24	0.026 ± 0.009
	16:04	27°50′22"S 26°40′26" E	0.52 ± 0.69	0.52 ± 0.20	0	0.32 ± 0.17	8.38 ± 0.21	0.039 ± 0.021
Day 5 27–08-2017 Downwind	08:02	27°50′11"S 26°40′4" E	15.3 ± 2.3	3.35 ± 0.42	0	3.33 ± 0.46	19.88 ± 0.32	0.168 ± 0.023
	08:50	27°50′14"S 26°40′2" E	11.4 ± 1.9	2.03 ± 0.32	0	2.24 ± 0.37	8.31 ± 0.21	0.269 ± 0.045
	09:43	27°50′18"S 26°40′0" E	6.7 ± 1.5	1.05 ± 0.26	0	1.24 ± 0.31	8.13 ± 0.20	0.152 ± 0.038
Upwind	11:51	27°49′30"S 26°39′56" E	5.08 ± 1.19	0.60 ± 0.22	0	0.84 ± 0.24	7.00 ± 0.19	0.121 ± 0.034
	13:01	27°49′27"S 26°40′54" E	2.84 ± 0.92	0.68 ± 0.21	0	0.65 ± 0.20	7.91 ± 0.20	0.082 ± 0.026
	13:50	27°49′26"S 26°39′51" E	0.84 ± 0.68	0	0	0.09 ± 0.07	5.69 ± 0.17	0.016 ± 0.012
	14:39	27°49′25"S 26°39′47" E	1.94 ± 0.83	0.75 ± 0.21	0	0.59 ± 0.19	7.25 ± 0.19	0.081 ± 0.027

very low. RaC can only be seen after 20 min of counting, but due to low radon activities, its activity after 20 min becomes too low. The other possibility could be that the measured radon was too "fresh", meaning that RaC has not had time to grow in the atmosphere. This is a possible indication that the "fresh" radon comes from the tailings.

Overall, the outdoor F factors were rather low compared to the adopted outdoor values of 0.6 by ICRP and 0.8 by UNSCEAR. Measurements at different receptor points from the tailings showed variations of the F factor reaching a factor of about 40 between the minimum and the maximum. The lowest values were less than 0.02 and occurred from midday to sunset whilst the highest ones reached 0.5 during the mid-morning. This has been verified by many surveys involving outdoor radon daughter measurements (Raviart et al. 1996). The variability of F factor values with environmental conditions, time, place, etc., implies that it is not recommended to always adopt the average recommended value for dose assessment purposes (Chen and Harley 2018). In addition, the use of the F factor alone to evaluate radon "age" and to isolate different possible contributors would not be adequate and that better interpretation would be attained from the individual radon daughters. More detailed analysis and interpretation of these results are presented in Section "Downwind morning results"–"Upwind results" below.

The uncertainty of the individual radon decay products, the EEC and F factor measurements was calculated and reported based on both Type A and Type B errors. The relative uncertainties for radon progeny measurements were relatively high at low activity concentrations, consistent with alpha particle counting at low environmental levels. RaC concentrations were so low that they were mostly regarded as undetectable. For a RaC value of zero, the RaC error did not contribute to the relative uncertainty for both the EEC and F factor. It is inherent and unavoidable with environmental alpha counting to expect low alpha count rates in the low particle concentration environment.

Downwind morning results

Radon and daughter Bateman calculations in Table 2 for day 1 morning downwind results predicted very high F factors compared to the measured ones, increasing from 0.50 at point A to 0.85 at point C, which is in contrast with the decreasing and low F factor from measured quantities in Table 1. These calculated values did not consider other external factors like meteorological conditions, wind direction, and wind speed, which affects dispersion (dilution) of radon and radon progeny in the atmosphere through air mixing. The only determining factor was the natural decay properties of half-life and decay constants.

In Fig. 5I, II, measured values of downwind radon concentrations, individual radon daughter concentrations and the F factors as function of distance and time are presented.

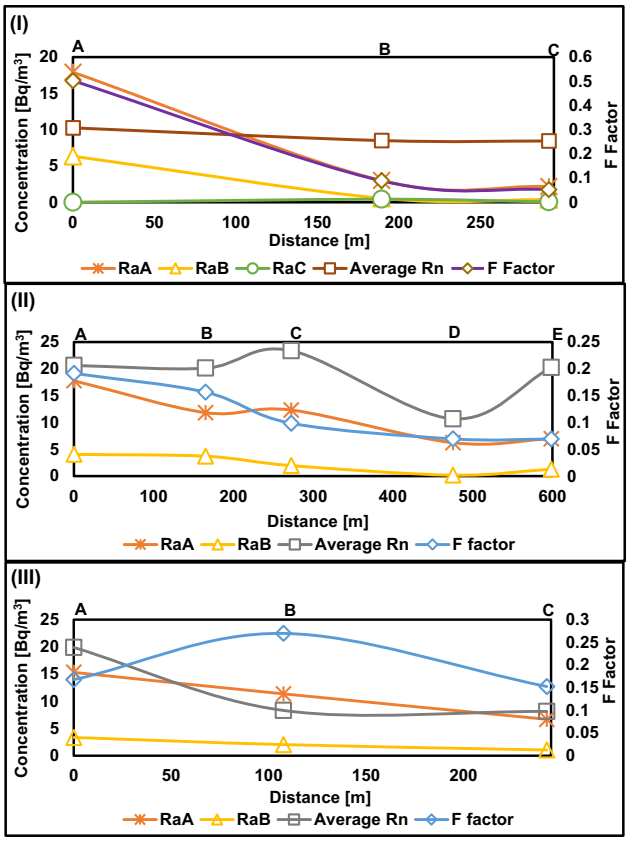

Fig. 5 Morning downwind Rn, RaA, RaB and RaC concentrations and F factor as function of distance from the tailing as measured on (**I**) day 1, (**II**) day 3 and (**III**) day 5

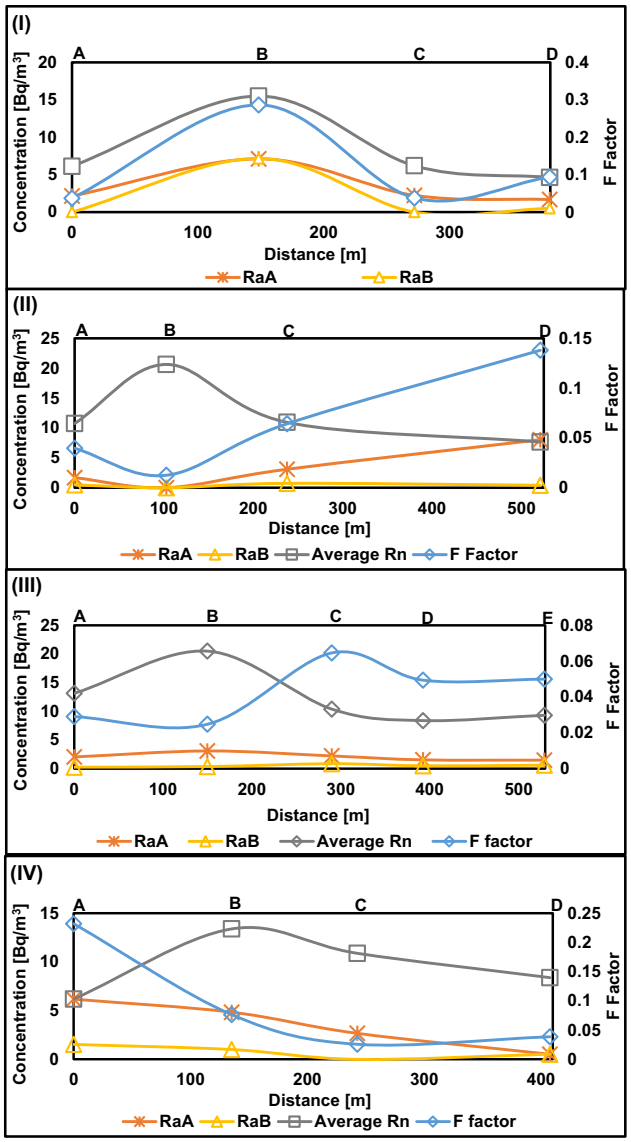

Fig. 6 Afternoon downwind for Rn, RaA and RaB concentrations and F factor as function of distance from the tailing as measured on (**I**) day 1, (**II**) day 2, (**III**) day 3 and (**IV**) day 4

Predominant wind directions were north–north-east in day 1 and 3 and north–north-west in day 5.

There is correlation between radon progeny in air with wind direction and speed (Doering 2019). This is shown by higher concentrations of radon progeny in air, specifically RaA, at point A for the three downwind morning measurements. The presence of high RaA and RaB activities signalled the presence of "old" and predominantly local gas that may have built up close to the tailings during the night, and not dispersing due to low wind. The simultaneous elevation in both radon and RaA activity concentrations at point A in Fig. 5II and Fig. 5III can be associated with low wind speed, positive temperature gradient, weak mixing and stable atmosphere, which is common during the night and in the early morning hours (Porstendörfer 1994; Hu and Tan 2000; Winkler et al. 2001; Porstendörfer and Gründel 2005). Radon concentration at point A in Fig. 5I was expected to be low due to the relatively high wind speed of 6.6 m/s at this point as compared to B (6.1 m/s) and C (5.6 m/s), yet this was not the case. This observation can be ascribed to the location characteristics at that point. Point A is surrounded by trees, and it is the closest to the dam, both of which act as wind shields. Therefore, the wind speed at that point may have been reduced, thus trapping radon gas at that point over time, and in the process decaying to produce RaA and elevated RaB.

A common pattern observed in day 1 and day 5 results emerged, which revealed that radon, RaA, RaB decreased from points A to C with time and distance, albeit relatively small changes in radon concentrations were observed. Radon continued to decay and some of the radon and radon daughters got diluted in air as the wind speed increased and temperature rises, leading to increased F factor from A to B on day 5 by 60.8% from 0.168 ± 0.023 to 0.269 ± 0.045. The F factor on day 1 decreased from point A to point C by

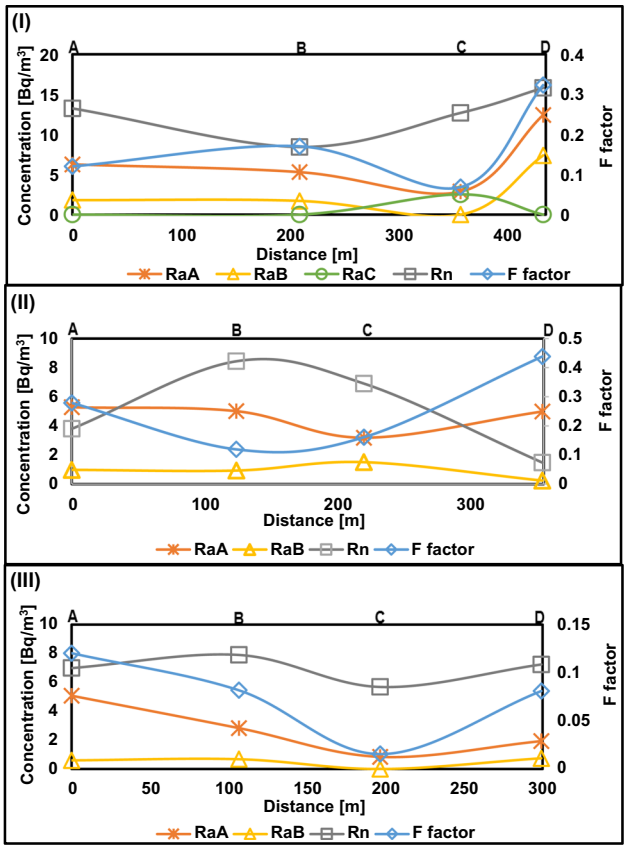

Fig. 7 Variation of upwind Rn, RaA, RaB, RaC concentrations, and F factors with distance from the tailing measured on (**I**) day 2 morning, (**II**) day 4 morning and (**III**) day 5 afternoon

a factor of 9, which is indicative of atmospheric disequilibrium between the parent radon and its daughter due to atmospheric mixing. As such, the radon at points B and C on day 1 can be considered to be predominantly of local origin, and not the radon transported by wind from other sources, whereas the air at point A may be due to mixing of "fresh" air from the dam and "old" air from other sources in the north-east direction.

A spike in radon concentration at point C on day 3 results (Fig. 5II) from 20.13 ± 0.32 Bq/m^3 to 23.38 ± 0.34 Bq/m^3 is evidence that there was another contributing radon source from some distant background source in the north–north-east direction or that was locally exhaled due to topographical conditions at that point. The slight RaA increase is due to the influence of "old" radon dispersed from other distant sources that continues to decay with time and distance. At point D, unsteady conditions of higher wind speeds (5.2 m/s) varied wind direction between 328.0° (north–north-west) and 0.5° (north), vertical mixing or wind shear caused dilution of radon in surface air, thus decreasing the number of radon daughters and F factor. The sharp radon activity increase and moderate increase in both RaA and RaB from point D to E show that the radon at point E is a mixture of the "old" local radon and "fresh" radon transported from the surroundings. The F factor remained unchanged.

Overall, radon concentrations, and hence radon progeny, were high at points A, C and E which were subjected to the north–north-east winds. Therefore, it is reasonable to conclude that winds from north–north-east and not from the tailings dam, contributed to excess radon at those receptor points.

Downwind afternoon results

Contrary to the morning patterns described above, a different trend emerged in the afternoon results. A common trend at point A shown in the afternoon results in Fig. 6I–III reveals high radon activity compared to RaA and RaB and low F factor due to low RaA and RaB ingrowth from parent decay. The lower afternoon radon concentration compared to the morning could be due to negative temperature gradient, even though the wind speed was less compared to that in the morning due to additional shielding provided by the tailings and vegetation around that point. Therefore, the air at point A in the three cases can be considered a mixture of "fresh" gas from both some distant background and local origin as well as "old" gas of local origin after having decayed and simultaneously producing daughters. Generally, lower F factor values indicate that the radon at that point is "fresh", having had limited transport and small build-up time for the radon daughters to be accumulated.

The wind speed at point A on day 3 was the highest for the afternoon, peaking at 4.2 m/s and the wind direction fluctuated by about 46°, characterising unstable conditions, thus yielding a diluted gas with strong vertical mixing.

From Fig. 6IV, it shows that at point A, the concentrations of radon and that of RaA were almost equal. However,

Table 2 Day 1 morning (downwind) Bateman calculated activities of radon, radon daughters and F factor as functions of distance and time for the downwind trend

Distance (m)	Time (s)	RaA (Bq/m^3)	RaB (Bq/m^3)	RaC (Bq/m^3)	Rn (Bq/m^3)	F factor
0 (Point A)	0	17.91	6.35	0	10.25	0.50
189.2 (Point B)	28.65	17.12	6.49	0.11	10.25	0.51
291.8 (Point C)	2.88E3	10.19	9.39	7.22	10.19	0.85

the concentration of RaB was about 4 times less than both radon and RaA. In this instance, the gas can be considered to be very "old", noting that this is the lowest downwind radon concentration to be measured in the five days of sampling, both in the morning and afternoon. The F factor was expected to be considerably higher at point A than the obtained value of 0.232 ± 0.042. This deviation from the expected trend has been observed before by Momeni et al. (1979).

From point A to point B, a characteristic radon "bump" is observed on all afternoon results. There are several possibilities to this sudden increase in radon at point B. One possibility is that the excess radon was transported from the northern direction by wind and air mass, given that the wind direction was fluctuating between north and north-east at point A and B in Fig. 6I, II and fluctuating between west and west-north-west in Fig. 6III, IV. Another possibility is that at about 100 m from the tailings dam, there was high radon exhalation from the local soil and strong vertical mixing conditions around that area. In addition, the rise of the dispersion plume due to the rising temperature during the day might have caused the plume to be higher, and it might first "hit" the ground at some downwind distance, causing the "bump" in the distance graph. Increased RaA and RaB at point B on day 1, 2 and 3 might be due to continued decay of local radon. The decreased F factor is an indication that the gas is disproportionately mixed, with high quantity of "fresh" radon exhaled from the soil and transported from other distant sources and a very small amount from the "old", decayed radon. The 67% drop in the F factor in Fig. 6IV at point B represent a decrease in radon daughter concentrations due to continued decay and deposition with increasing radon gas.

One notable observation on day 1 is a close resemblance between point C and point A in terms of radon concentration, RaA, RaB and the F factor. Even though the wind speed at point C was the highest at 3.5 m/s as compared to 3.1 m/s at point A, the dominating wind direction at both points is the north–north-east winds. It therefore follows that the two points were subjected to the same external radon source. Furthermore, radon and radon daughters decrease with time and increasing distance from the tailings due to atmospheric dilution, confirming the observation by Momeni et al. (1979) and Molchanov et al. (2010).

Upwind results

From Fig. 7I, II, III, the highest radon concentrations were measured on day 2. The wind speeds corresponding to point A and B were 6.2 m/s and 6.1 m/s, respectively. The wind direction fluctuated between 33.4°. (north–north-east) and 35.8° (north–north-east) at point A, 17.85° (north–north-east) and 25.7° (north–north-east) at point B, 1.8° (north) and 20.0° (north–north-east) at point C and 5.6° (north) and 10.1° (north) at D.

The F factor value of 0.12 indicates a mixture of "fresh" local radon and "old" gas from some distant background at point A. Point D had the highest activity of radon, RaB as well as the F factor, indicating enough build-up time for the radon daughters to be accumulated. The emergence of RaC in point C was due to the continuous decay of RaA, whereas the increase in RaA, RaB and the F factor from C to D is partly due to the "old" decaying radon and the mixed gas from the northern direction.

One notable observation in Fig. 7II, III is that there was a characteristic radon "bump" from point A to point B. In both cases, there was a decrease in the wind speed from 9.9 m/s at point A to 8.3 m/s at point B in Fig. 7II and from 3.4 to 2.9 m/s in Fig. 7III, thereby reducing the dilution factor and thus increasing the radon concentration at B. This was accompanied by a corresponding decrease in the F factor, representing a decrease in activity of radon daughters. It can be further observed in Fig. 7II and Table 1 that from point A to point B, RaA and RaB decreased almost in the same way as the normal decay with time shown in Table 2.

Overall, there were no significant differences between the upwind and downwind results. In some instances, the concentrations of radon and radon progeny in downwind directions were less than the upwind concentrations. This means that any radon progeny in air due to atmospheric radon transport from tailings dam was undetectable above background. Consequently, the environmental impact of radon from the tailings dam on the surrounding area was small considering these results include the natural background component. Therefore, the tailings-related radon progeny concentrations used for radiation exposure and dose estimates are considered to be very low.

It is noteworthy to point out that there were some significant increases in radon and radon daughter activities observed in the downwind measurements that were mostly influenced by wind transported radon from the north–north-east direction and to a lesser extent the north–north-west directions. Therefore, it was radon and progenies that were transported from distant sources that increased the ambient radon and radon progeny activities around the tailings dam, albeit small and well below the action reference level for the dose to a member of the public of less than 1 mSv/y and radon concentration level of 100 Bq/m^3 as prescribed by WHO.

Conclusion

Isolating different radon contributors in the vicinity of a tailings dam is an important aspect of assessing radiological impact on the public due to the atmospheric release and

transport of radon from the tailings dams. This study postulated that the "follow the wind" approach will provide a more pronounced interpretation of the values of radon and radon progeny concentrations and the F factor in terms of identifying and deducing the "age" of the gas compared to the "age" of the background sources.

The study has highlighted the effect of external meteorological effects on the distribution of radon and radon daughters some distance from the tailings and background. The results confirmed that activity concentrations of radon and its daughters do not remain constant even under same distances from a tailings or same wind speeds. Concentration changes by radioactive decay were overshadowed by other factors. Their magnitudes change with changing wind direction and local conditions of exhalation. Considering the downwind results, on average, the radon activity increased at distances ranging from 100 m to about 150 m from the base of the tailings at point A. This effect, depicted by "bumps" in Fig. 6I, II, III, IV, was consistent in all afternoon results. The predominant wind direction accompanying most radon concentration increases, including the 162% highest radon increase from point A to point B observed on day 4 was mainly from north–north-east. In addition, the F factor (on average) attained its highest value when the wind was blowing from north–north-east, while its lowest value and smallest change were obtained when the wind was blowing from west-north-west. The highest radon daughter concentrations which varied with location were recorded in the mornings. On the upwind, the highest radon activity was 15.81 ± 0.28 Bq/m^3 for the wind blowing from the northern direction at point D further away from the dam, with the lowest value coming from the west-north-west direction. Overall, radon and radon progeny concentrations and the F factor decreased from point D (away from the tailings) to point A (closer to the tailings).

Different meteorological conditions presented fluctuations and conflicting effects on atmospheric radon, radon daughters and hence the F factor activities as functions of distance from the tailings downwind. The absence of a clear pattern over the study period was an indication that variations in outdoor radon and short-lived progeny concentrations are strongly guided by atmospheric dispersion conditions. This experience shows that air dispersion modelling will be very useful to explain the results further. However, taking everything into account, the study revealed that the tailings contribution to the background radon concentration was found to be minimal.

Acknowledgements Special thanks to Harmony Gold Mining Company Limited for permission to access their facility, the late Dirk Venter (MHSRIP) for logistical and technical support, EDTP SETA and Sol Plaatje University (Kimberley), Prof Victor Tshivhase and Prof Manny Matutu at the Centre for Applied Radiation Science and Technology (CARST), North West University for your support and for providing us with your equipment, Motheo Security (Welkom) and Sol Plaatje University Staff and 2018 third-year Data Science Students.

Declarations

Conflict of interest The authors have no relevant financial or non-financial interests to disclose.

References

Akber R, Pfitzner J (1994) Atmospheric concentrations of radon and radon daughters in Jabiru East. Supervising Scientist for The Alligators Region, Canberra

Arnold D, Vargas A, Ortega X (2009) Analysis of outdoor radon progeny concentration measured at the Spanish radioactive aerosol automatic monitoring network. Appl Radiat Isot 67:833–838. https://doi.org/10.1016/j.apradiso.2009.01.042

ATSDR (2012) Toxicological profile for radon. Agency for Toxic Substances and Disease Registry, Atlanta, GA

Baciu AC (2005) Radon and thoron progeny concentration variability in relation to meteorological conditions at Bucharest (Romania). J Environ Radioact 83:171–189. https://doi.org/10.1016/j.jenvrad.2005.02.015

Bateman H (1910) The solution of a system of differential equations occurring in the theory of radioactive transformations. Proc Camb Philos Soc 15:423–427

Bersimbaev RI, Bulgakova O (2015) The health effects of radon and uranium on the population of Kazakhstan. Genes Environ 37:18. https://doi.org/10.1186/s41021-015-0019-3

Blaauboer RO, Smetsers RCGM (1997) Outdoor concentrations of the equilibrium-equivalent decay products of 222Rn in the Netherlands and the effect of meteorological variables. Radiat Prot Dosimet 69:7–18. https://doi.org/10.1093/oxfordjournals.rpd.a031889

Busigin A, Phillips CR (1980) Uncertainties in the measurement of airborne radon daughters. Health Phys 39:943–955. https://doi.org/10.1097/00004032-198012000-00008

Čeliković I, Pantelić G, Vukanac I et al (2022) Outdoor radon as a tool to estimate radon priority areas—a literature overview. Int J Environ Res Public Health 19:662. https://doi.org/10.3390/ijerph19020662

Chambers S, Williams A, Crawford J, Griffiths A (2014) On the use of radon for quantifying the effects of atmospheric stability on urban emissions. Atmos Chem Phys 14:25411–25452. https://doi.org/10.5194/acpd-14-25411-2014

Chen J, Harley NH (2018) A review of indoor and outdoor radon equilibrium factors-part I: 222Rn. Health Phys 115:490–499. https://doi.org/10.1097/HP.0000000000000909

Chen J, Marro L (2011) Assessment of radon equilibrium factor from distribution parameters of simultaneous radon and radon progeny measurements. Radiat Environ Biophys 50:597–601. https://doi.org/10.1007/s00411-011-0375-8

Chen J, Moir D, Whyte J (2012) Canadian population risk of radon induced lung cancer: a re-assessment based on the recent cross-Canada radon survey. Radiat Prot Dosimet 152:9–13. https://doi.org/10.1093/rpd/ncs147

Climate-Data.org (2019) Odendaalsrus climate: Average Temperature, weather by month, Odendaalsrus weather averages - Climate-Data.org. https://en.climate-data.org/africa/south-africa/free-state/odendaalsrus-26385/. Accessed 1 Aug 2019

Darby S, Hill D, Auvinen A et al (2005) Radon in homes and risk of lung cancer: collaborative analysis of individual data from 13

European case-control studies. BMJ 330:223. https://doi.org/10.1136/bmj.38308.477650.63
de Paula VM, de Sá LV, Braz D (2020) Comparative analysis of equipment performance in nuclear medicine. Braz J Radiat Sci 8:993. https://doi.org/10.15392/bjrs.v8i1B.993
Degu Belete G, Alemu Anteneh Y (2021) General overview of radon studies in health hazard perspectives. Journal of Oncology 2021:e6659795. https://doi.org/10.1155/2021/6659795
Deyuan T (1991) Analysis of radon-222 daughters in air. J Radioanal Nucl Chem 154:5–21
Doering C (2019) A new background subtraction method for assessing public radiation exposure due to radon transport from a uranium mine. Radiat Prot Dosimet 186:530–535. https://doi.org/10.1093/rpd/ncz141
Field RW (2018) Radon: a leading environmental cause of lung cancer. afp 98:280–282
Furuta S, Ito K, Ishimori Y (2002) Measurements of radon around closed uranium mines. J Environ Radioact 62:97–114. https://doi.org/10.1016/s0265-931x(01)00154-0
Saphymo GmbH (2012) Portable radon monitor, User Manual
Habib RR, Nuwayhid RY, Hamdan Z et al (2018) Indoor and outdoor radon concentration levels in Lebanon. Health Phys 115:344–353. https://doi.org/10.1097/HP.0000000000000888
Hu SJ, Tan KS (2000) Radon and its progeny in outdoor air. ASEAN J Sci Technol Dev 17:65–70. https://doi.org/10.29037/ajstd.122
IAEA (1991) Quality control of nuclear medicine instruments. International Atomic Energy Agency, Vienna
IARC (1988) Man-made mineral fibres and radon
ICRP (2009) Statement on radon. International Commission on Radiological Protection, Ottawa
JCGM (2008) Evaluation of measurement data—Guide to the expression of uncertainty in measurement. Int Organ Stand Geneva ISBN 50:134
Kang JK, Seo S, Jin YW (2019) Health effects of radon exposure. Yonsei Med J 60:597–603. https://doi.org/10.3349/ymj.2019.60.7.597
Komati FS (2020) Radon dispersion from a south african gold mine-tailings dam—measurement and modelling. Central University of Technology, Bloemfontein, PhD
Kumar KC, Prasad TR, Ratnam MV, Nagaraja K (2016) Activity of radon (222Rn) in the lower atmospheric surface layer of a typical rural site in south India. J Earth Syst Sci 125:1391–1397. https://doi.org/10.1007/s12040-016-0745-3
Leach VA, Chandler WP (1992) Atmospheric dispersion of radon gas and its decay products under stable conditions in arid regions of Australia. Environ Monit Assess 20:1–17. https://doi.org/10.1007/BF00396516
Lindsay R, de Meijer RJ, Joseph AD et al (2004) Measurement of radon exhalation from a gold-mine tailings dam by γ-ray mapping. Radiat Phys Chem 71:797–798. https://doi.org/10.1016/j.radphyschem.2004.04.097
Lindsay R, Newman RT, Speelman WJ (2008) A study of airborne radon levels in Paarl houses (South Africa) and associated source terms, using electret ion chambers and gamma-ray spectrometry. Appl Radiat Isot 66:1611–1614. https://doi.org/10.1016/j.apradiso.2008.01.022
Lubin JH, Wang ZY, Boice JD Jr et al (2004) Risk of lung cancer and residential radon in China: Pooled results of two studies. Int J Cancer 109:132–137. https://doi.org/10.1002/ijc.11683
Maiello ML, Hoover MD (eds) (2010) Radioactive air sampling methods. CRC Press, Boca Raton
Michelin (2022) MICHELIN Kutlwanong map - ViaMichelin. https://www.viamichelin.com/web/Maps/Map-Kutlwanong-9480-Vryst aat-South_Africa. Accessed 3 Aug 2022
Molchanov O, Soroka Yu, Podrezov A et al (2010) Dispersion of radon in the atmosphere around old uranium mill tailings. Nukleonika 55:535–538
Momeni MH, Lindstrom JB, Dungey CE, Kisieleski WE (1979) Radon and radon-daughter concentrations in air in the vicinity of the Anaconda Uranium Mill
Moshupya P, Abiye T, Mouri H et al (2019) Assessment of radon concentration and impact on human health in a region dominated by abandoned gold mine tailings dams: a case from the West Rand region. S Afr Geosci 9:466. https://doi.org/10.3390/geosciences9110466
Neuberger J, Harley N, Kross B (1996) Residential radon exposure and lung cancer: potential for pooled or meta-analysis. J Clean Technol Environ Toxicol Occup Med 5:207–221
Ongori JN, Lindsay R, Newman RT, Maleka PP (2015) Determining the radon exhalation rate from a gold mine tailings dump by measuring the gamma radiation. J Environ Radioact 140:16–24. https://doi.org/10.1016/j.jenvrad.2014.10.012
Podstawczyńska A, Kozak K, Pawlak W, Mazur J (2010) Seasonal and diurnal variation of outdoor radon (222Rn) concentrations in urban and rural area with reference to meteorological conditions. Nukleonika 12:543–547
Porstendörfer J (1994) Properties and behaviour of radon and thoron and their decay products in the air. J Aerosol Sci 25:219–263. https://doi.org/10.1016/0021-8502(94)90077-9
Porstendörfer J, Gründel M (2005) Radon decay products in outdoor air. In: Radioactivity in the Environment. pp 56–65
Pressyanov DS, Guelev MG, Sharkov BG (1995) Radon and radon progeny outdoors in a valley of enhanced natural radioactivity. Atmos Environ 29:3433–3439. https://doi.org/10.1016/1352-2310(95)00204-c
Raviart S, Richon P, Haristoy D et al (1996) Field determination of the time-varying equilibrium factor between 222Rn and its short-lived decay products in the atmosphere above a waste-rock pile. Environ Int 22:279–286. https://doi.org/10.1016/S0160-4120(96)00119-5
Rozas S, Idoeta R, Alegría N, Herranz M (2016) Radiological characterisation and radon equilibrium factor in the outdoor air of a post-industrial urban area. J Environ Radioact 151:126–135. https://doi.org/10.1016/j.jenvrad.2015.09.023
Siaway G, Mose D, Metcalf J (2009) Evaluation of indoor radon potential in northern virginia using spacial autocorrelation. Gis Appl 3D Vis 14:27
Singh K, Singh M, Singh S et al (2005) Variation of radon (222Rn) progeny concentrations in outdoor air as a function of time, temperature and relative humidity. Radiat Meas 39:213–217. https://doi.org/10.1016/j.radmeas.2004.06.015
Song J-M, Kim W-H, Kang C-H et al (2015) Temporal variability of atmospheric radon-222 concentration at Gosan Station, Jeju Island, Korea, during 2009–2013. Bull Korean Chem Soc 36:603–608. https://doi.org/10.1002/bkcs.10118
Speelman WJ (2004) Modelling and measurement of radon diffusion through soil for application on mine tailings dam. University of the Western Cape, MSc
Tchorz-Trzeciakiewicz DE, Solecki AT (2018) Variations of radon concentration in the atmosphere. Gamma Dose Rate Atmos Environ 174:54–65. https://doi.org/10.1016/j.atmosenv.2017.11.033
Thomas JW (1972) Measurement of radon daughters in air. Health Phys 23:783–789. https://doi.org/10.1097/00004032-197212000-00004
Thompson RE (2014) Radon. In: Wexler P (ed) Encyclopedia of toxicology, 3rd edn. Academic Press, Oxford, pp 46–50
UNSCEAR (2000) Sources and effects of ionizing radiation. UN
UNSCEAR (2008) Sources and effects of ionizing radiation, UNSCEAR Report to the general assembly, with scientific annexes; United Nations
WHO (2009) WHO Handbook on Indoor Radon: A Public Health Perspective. World Health Organization, Geneva
Windfinder.com (2019) Windfinder.com - Wind and weather statistic Welkom Airport. In: Windfinder.com. https://www.windfinder.com/windstatistics/welkom. Accessed 1 Aug 2019

Winkler R, Ruckerbauer F, Trautmannsheimer M et al (2001) Diurnal and seasonal variation of the equilibrium state between short-lived radon decay products and radon gas in ground-level air. Radiat Environ Biophys 40:115–123. https://doi.org/10.1007/s004110100096

Zhang L, Wang Y, Gou Q (2020) One-year continuous measurement of outdoor radon progeny concentration in Beijing area. J Radiat Protect Res 45:95–100